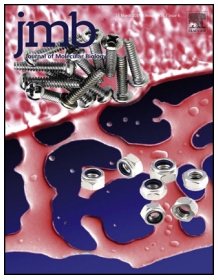

Yeast Two-Hybrid Analysis for Ubiquitin Variant Inhibitors of Human Deubiquitinases

Natasha Pascoe[1,2], Ashwin Seetharaman[2], Joan Teyra[2], Noah Manczyk[3,4], Maria Augusta Satori[2], Donna Tjandra[1,2], Taras Makhnevych[2], Carsten Schwerdtfeger[5], Bradley B. Brasher[5], Jason Moffat[1,2,6], Michael Costanzo[2,6], Charles Boone[1,2,6], Frank Sicheri[1,3,4] and Sachdev S. Sidhu[1,2,3]

1 - Department of Molecular Genetics, *University of Toronto, Toronto, ON M5S 3E1, Canada*
2 - Donnelly Centre for Cellular and Biomolecular Research, *Banting and Best Department of Medical Research, University of Toronto, Toronto, ON, M5S3E1, Canada*
3 - Department of Biochemistry, *University of Toronto, Toronto, ON M5S 1A8, Canada*
4 - Lunenfeld–Tanenbaum Research Institute, *Mount Sinai Hospital, 600 University Avenue, Toronto, ON M5G 1X5, Canada*
5 - Boston Biochem, *a Bio-Techne Brand 840 Memorial Drive, Cambridge, MA 02139, USA*
6 - Canadian Institute for Advanced Research, *Toronto, ON, M5G1Z8, Canada*

Correspondence to Sachdev S. Sidhu: *Department of Molecular Genetics, University of Toronto, Toronto, ON M5S 3E1, Canada. sachdev.sidhu@utoronto.ca.*
https://doi.org/10.1016/j.jmb.2019.02.007
Edited by S. Koide

Abstract

We applied a yeast-two-hybrid (Y2H) analysis to screen for ubiquitin variant (UbV) inhibitors of a human deubiquitinase (DUB), ubiquitin-specific protease 2 (USP2). The Y2H screen used USP2 as the bait and a prey library consisting of UbVs randomized at four specific positions, which were known to interact with USP2 from phage display analysis. The screen yielded numerous UbVs that bound to USP2 both as a Y2H interaction *in vivo* and as purified proteins *in vitro.* The Y2H-derived UbVs inhibited the catalytic activity of USP2 *in vitro* with nanomolar-range potencies, and they bound and inhibited USP2 in human cells. Mutational and structural analysis showed that potent and selective inhibition could be achieved by just two substitutions in a UbV, which exhibited improved hydrophobic and hydrophilic contacts compared to the wild-type ubiquitin interaction with USP2. Our results establish Y2H as an effective platform for the development of UbV inhibitors of DUBs *in vivo*, providing an alternative strategy for the analysis of DUBs that are recalcitrant to phage display and other *in vitro* methods.

Introduction

The Ubiquitin Proteasome System (UPS) regulates numerous cellular processes through effects on protein localization and degradation [1,2]. Recent advances have identified components of the UPS as promising therapeutic targets [1,2]. Indeed, targeting the UPS has been successful, with a key example being the use of the proteasome inhibitor bortezomib for the treatment of multiple myeloma [3,4]. However, a consequence of global UPS inhibition by bortezomib is extensive cytotoxicity, which limits its therapeutic potential. As such, inhibitors targeting other components of the UPS may enhance specificity and efficacy, and could thus improve therapeutic outcomes for patients [3,4,5–7].

Deubiquitinating enzymes (DUBs) catalyze the removal of ubiquitin (Ub) from target substrates and affect a wide variety of cellular processes by influencing the localization, stability and function of their substrates [1,2]. Inhibition of DUB activity has emerged as a promising therapeutic strategy to treat several diseases including various cancers and neurodegenerative diseases [7,8,9]. Despite this, there is a paucity

of specific and potent inhibitors of DUBs, which has hindered attempts to exploit them for therapeutic benefit. To address this issue, our group developed a strategy employing Ub as a scaffold to engineer potent and specific DUB inhibitors, called Ub variants (UbVs) [10–12]. We have previously reported the generation of massively diverse combinatorial libraries containing billions of unique UbVs, and we have used *in vitro* phage display selections to identify inhibitors of several different proteins in the UPS [13].

Ubiquitin-specific protease 2 (USP2) is a human DUB that is involved in the regulation of cell cycle progression and cell death, and it has recently emerged as a potential therapeutic target for several diseases including prostate and triple-negative breast cancer [14–16]. Phage display library screens have yielded several UbVs capable of binding and inhibiting the function of USP2 *in vitro*, and substitutions at four positions in the N-terminal region of Ub (positions 2, 6, 11 and 12) are sufficient for the generation of potent and specific UbV inhibitors of USP2 [11,12].

However, while these UbVs inhibited USP2 activity *in vitro,* they failed to interact with USP2 in human cells, possibly suggesting poor stability, improper folding, reduced affinity and/or specificity for their target *in vivo*. This issue may be a general concern because UbV binding affinities and specificities observed *in vitro* do not always hold true *in vivo*. Moreover, it can be challenging to purify DUBs, which is a prerequisite for *in vitro* phage display. On the other hand, *in vivo* screening systems more accurately reflect cellular conditions and do not require purified proteins as targets. Thus, *in vivo* screening systems could circumvent some of the limitations inherent to *in vitro* strategies to provide complementary methodology for the production of DUB inhibitors.

In particular, the yeast-two-hybrid (Y2H) analysis is a well-established and powerful approach for identifying protein–protein interactions *in vivo* [17,18]. Here, we tested Y2H as an effective platform for the discovery of UbV inhibitors of human DUBs. We constructed a complex Y2H prey library comprising UbVs and showed that USP2 baits can be used to identify UbVs that are capable of binding and inhibiting USP2 in human cells. These results highlight the power of an *in vivo* approach for the discovery of novel UbV reagents.

Results

Y2H is an effective intracellular platform for detecting DUB–UbV interactions

We sought to establish a Y2H as an *in vivo* assay to develop UbV inhibitors of DUBs. Using phage display, we previously identified UbVs capable of binding components of the UPS, including two UbVs that targeted USP2 (UbV.2.1^{PH} and UbV.2.11^{PH}, where "PH" indicates UbVs derived by phage display) [11,12]. To determine whether interactions between USP2 and phage-derived UbVs could be detected *via* Y2H analysis, we made constructs that expressed USP2, either as a full-length protein (USP2^{FL}) or as a C-terminal catalytic domain (USP2^{Cat}, comprising of residues 262–605) [11], as a Gal4 DNA binding domain (DBD) bait fusion protein or as a Gal4 activation domain (AD) prey fusion protein. Similarly, we generated bait and prey constructs with wild-type Ub (Ub.wt) and a series of phage-derived UbVs that targeted USP2, including UbV.2.3^{PH}, UbV.2.7^{PH}, UbV.2.9^{PH} and UbV.2.11^{PH}. These Y2H constructs were transformed into a reporter yeast strain (Y15409), such that each DUB bait construct was co-expressed with its cognate UbV, Ub.wt or a control plasmid. Protein–protein interactions were inferred from the expression of two distinct reporter genes, *HIS3* and *yEGFP*, which can be detected by growth on media lacking histidine or through enhanced green fluorescent protein (EGFP) fluorescence, respectively. In addition, the stringency of *HIS3* selection can be increased through the addition of a competitive inhibitor of the *HIS3* gene product, 3-amino triazole (ATZ) [19].

The combination of a USP2^{FL} bait and Ub.wt prey resulted in weak *HIS3* reporter expression, which could be eliminated by increasing the selection stringency with ATZ. Notably, we found that USP2^{FL} bait activated the *HIS3* reporter strongly in the presence of UbV.2.1^{PH} prey, suggesting that these two proteins bind tightly in the Y2H context. We also detected reporter activation with USP2^{FL} bait and several different phage-derived UbV preys, including UbV.2.3^{PH}, UbV.2.7^{PH}, UbV.2.9^{PH} and UbV.2.11^{PH}, although none of these UbVs appeared to bind the USP2^{FL} bait as strongly as UbV.2.1^{PH}. Interestingly, we could not detect a Y2H interaction with other phage-derived UbVs (Supplementary Fig. 1A). Similarly, using the EGFP Y2H reporter and FACS analysis, we detected strong Y2H interactions between either the USP2^{Cat} or the USP2^{FL} bait with a UbV.2.1^{PH} prey, whereas no interaction was detected for Ub.wt prey (Supplementary Fig. 1B). Taken together, these results show that the Y2H analysis permits detection of interactions between USP2 and cognate UbVs; however, many UbVs that bound and inhibited USP2 *in vitro* failed to detectably bind USP2 *in vivo*.

Y2H library screens yield potent, specific and stable UbV inhibitors of USP2

To facilitate the discovery of *in vivo* UbV binders for USP2, we generated a UbV library that was compatible with the Y2H screening platform. From

phage display analysis, we showed previously that residues at four positions [2,6,11,12] within the N-terminal region are particularly important for the generation of potent and specific UbV inhibitors of USP2 [11,12]. Thus, we generated a library of UbV prey constructs, in which these positions were diversified using a hard randomization strategy [20] with degenerate codons that allowed for all 20 genetically encoded amino acids in a combinatorial manner (Fig. 1a). The resulting library, consisting of 1.6×10^5 unique UbVs, was expressed in a Y2H reporter yeast strain (Y14568) that contained *URA3, HIS3, LacZ* and *yEGFP* reporters (see Materials and Methods).

We utilized the yeast mating system to generate diploid cells carrying both a USP2 bait plasmid and a UbV prey library plasmid. To isolate UbVs that bound USP2, the UbV prey library was mated to isogenic yeast strains of the opposite mating type that either expressed an untagged Gal4 DBD bait (control plasmid) or a USP2 bait. Resulting strains were first subjected to selection for *HIS3* expression in solution and subsequently collected and selected for EGFP expression by FACS. Screens with $USP2^{Cat}$ and $USP2^{FL}$ baits showed that EGFP was expressed in 0.41% and 0.15% of cells, respectively, while no cells expressed EGFP in screens against control plasmid (Supplementary Fig. 2A). Similar results were obtained with a higher-stringency *HIS3* selection, in which ATZ was included in the medium (Supplementary Fig. 2A). We further validated our results by re-transforming UbVs isolated from the $USP2^{FL}$ screens into yeast cells that expressed either the control plasmid or a $USP2^{FL}$ bait and assessed *GFP* reporter gene expression. This analysis showed that 98% of the UbVs isolated through our Y2H screens showed robust activation of the EGFP reporter gene (Supplementary Fig. 2B).

We sequenced 700 clones and identified 555 unique UbVs that were isolated as putative USP2 binders. Compared to UbVs selected through phage display, UbVs selected by Y2H were more variable but still retained some preference for sequences that resembled those selected previously [12] (Fig. 1b). However, unlike phage-derived UbVs, Y2H-derived UbVs exhibited a strong preference for cysteine at positions 2, 6 and 12. Similar UbV sequences were selected, regardless of whether $USP2^{FL}$ or USP^{Cat} was used as the bait, or *via* the use of *HIS3* and EGFP *repo*rters or *HIS3* alone (Fig. 1b). Proteins fused to phage coat proteins for phage display are secreted into the periplasm, where the oxidizing environment can cause cysteine residues to form

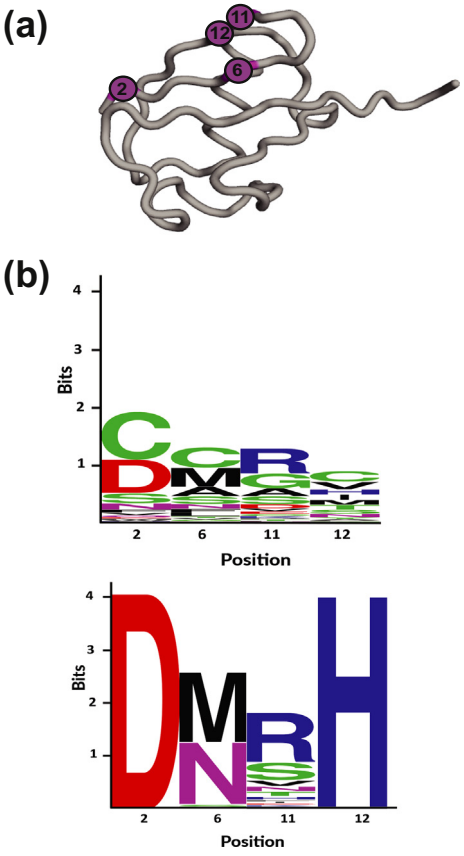

(c)

	Position 2	6	11	12	IC_{50} (nM)
Ub.wt	Q	K	K	T	100μM
UbV. 2.1^{PH}	Q	N	K	H	50 ± 10
UbV. 2.2	D	M	D	C	6 ± 1
UbV. 2.3	C	A	G	C	7 ± 2
UbV. 2.4	D	A	R	S	20 ± 5
UbV. 2.5	D	A	G	H	11 ± 0
UbV. 2.6	C	C	R	C	3 ± 0
Q2C	C	K	K	T	1900 ± 500
K6C	Q	C	K	T	100 ± 10
K11R	Q	C	R	T	60 ± 5
T12C	Q	C	K	C	500 ± 10
K6C/K11R	Q	C	R	T	20 ± 2

Fig. 1. UbVs derived by Y2H inhibit USP2 *in vitro*. (a) Y2H UbV library design. The main chain of Ub is depicted as a gray tube, and magenta spheres indicate positions that were varied as combinations of all 20 genetically encoded amino acids using NNK (N = A/G/C/T, K = G/T) degenerate codons. (b) Sequence logos derived from the relative amino acid frequencies for UbVs selected for binding to USP2 by Y2H (top, n = 700) or phage display (bottom, n = 96) using WebLogo™. (c) Sequence alignment and IC_{50} values of UbV inhibitors of USP2. The alignment shows only those positions that were diversified in the Y2H library, and positions that were conserved as the wild-type sequence are shown as dashes. IC_{50} values were determined as the concentration of UbV required to inhibit 50% of the activity of USP^{Cat} for hydrolysis of Ub-AMC.

non-native disulfides that can interfere with protein function. We speculate that cysteine residues in the phage-displayed libraries may have been depleted due to these complications, whereas Y2H in the reducing intracellular environment does not pose any challenges for proteins that contain cysteine residues.

To determine whether UbVs derived by Y2H were able to inhibit USP2 catalytic activity *in vitro*, we monitored the proteolytic activity of $USP2^{Cat}$ using the fluorogenic substrate Ub-AMC [11,12]. We tested the effects of five UbVs isolated in the Y2H screens, and as a positive control, we also analyzed $UbV.2.1^{PH}$, which was previously selected for binding to USP2 by phage display (Fig. 1c and Supplementary Fig. 3A). UbV.2.6, the most potent UbV derived by Y2H, contained three cysteine residues and inhibited $USP2^{Cat}$ activity with an IC_{50} value of 3 nM, and was thus more than an order of magnitude more potent than $UbV.2.1^{PH}$ (IC_{50} = 48 nM). To assess selectivity, we analyzed UbV.2.6 and $UbV.2.1^{PH}$ with *in vitro* proteolytic assays against a panel of 13 human DUBs (including USP21, the closest USP2 homolog) and observed strong inhibition only for USP2 (Table 1). To further assess selectivity and to explore the utility of Y2H analysis for the identification of specific UbV-DUB interactions, we cloned 29 USPs, 5 other DUBs and 6 E2 enzymes into a Y2H bait system and tested them for interaction with UbVs 2.2 and 2.6, and we found that only USP2 showed a strong positive Y2H interaction (Supplementary Fig. 4).

Lastly, we compared the stability of UbV.2.6 and $UbV.2.1^{PH}$ to that of Ub.wt, which is very thermostable, with a melting temperature greater than 100 °C at physiological pH [21]. At 37 °C, the three proteins exhibited virtually identical circular dichroism (CD) spectra consistent with a mixed α/β secondary structure (Supplementary Fig. 5A) [22], suggesting that they are all capable of folding in cells. Temperature denaturation showed that all three proteins remained folded at 90 °C (Supplementary Fig. 5A, B), and chemical denaturation experiments showed that all three proteins unfolded at a similar concentration of guanidinium hydrochloride (Supplementary Fig. 5C). These data show that the global fold and stability of the UbVs are similar to those of Ub.wt, and both the phage- and Y2H-derived UbVs should be stably folded at physiological temperature and pH. Taken together, our results show that Y2H is a robust *in vivo* platform for the identification of stable, potent and specific UbV inhibitors of USP2.

UbVs interact with and inhibit USP2 in human cells

Having established that UbVs 2.2 and 2.6 bind specifically to USP2 in yeast and inhibit its activity *in vitro,* we sought to determine whether the UbVs could interact with endogenous USP2 in human cells. We used transient transfections to express Flag-tagged UbVs in HEK293T cells, immunoprecipitated the UbVs with an anti-FLAG antibody, and assessed co-precipitation of endogenous USP2 by Western blotting with an anti-USP2 antibody. These experiments showed that UbVs 2.2 and 2.6 were able to co-immunoprecipitate USP2, whereas Ub.wt and $Ubv.2.1^{PH}$ failed to do so (Fig. 2a).

Having determined that UbVs 2.2 and 2.6 interact with endogenous USP2 in human cells, we investigated whether they could inhibit the intracellular activity of USP2. USP2 deubiquitinates the E3 ligase MDM2 and prevents its degradation [23], and thus, we explored the effects of UbVs on MDM2 ubiquitination. We transiently transfected HEK293T cells with plasmids to express Flag-tagged UbV.2.2 or UbV.2.6, MDM2 and HA-tagged Ub.wt in the presence of the proteasome inhibitor MG132. Western blotting revealed that expression of UbV.2.2 or UbV.2.6 resulted in significantly increased ubiquitination of MDM2 (Fig. 2b). Taken together, these results confirm that UbVs 2.2 and 2.6 function as inhibitors of USP2 in cells.

Mutational and structural analysis reveals the molecular basis for UbV function

To better understand the basis for the potent inhibition of USP2 by UbV.2.6, we introduced each of the four substitutions from UbV.2.6 individually into the sequence of Ub.wt and assessed effects on USP2 activity (Fig. 1c and Supplementary Fig. 3B). This analysis confirmed that each of the four substitutions substantially enhanced the potency of inhibition. The substitutions at positions 6 and 11 had the greatest effects, and indeed, a UbV bearing

Table 1. IC_{50} values for inhibition of DUB activity by UbVs

UbV	IC_{50} (nM)[a]												
	USP2	USP4	USP7	USP8	USP9x	USP11	USP15	USP19	USP21	USP28	USP30	UCHL3	UCHL5
2.1^{PH}	20 ± 3	800 ± 70	>1000	>1000	>1000	>1000	>1000	>1000	>1000	>1000	>1000	>1000	>1000
2.6	9.5 ± 0.5	900 ± 60	>1000	>1000	>1000	>1000	>1000	>1000	>1000	>1000	>1000	>1000	>1000

[a] The IC_{50} value was defined as the concentration of UbV required to inhibit 50% of the activity of the enzyme for hydrolysis of Ub-Rh110 substrate. Data are presented as the mean ± SD (n = 4).

substitutions at both positions was only 6-fold less potent than Ub.V.2.6.

To visualize the molecular basis for USP2 inhibition by UbV.2.6, we determined the crystal structure of UbV.2.6 in complex with $USP2^{Cat}$ at 2.34-Å resolution (Table 2). We found that UbV.2.6 bound to $USP2^{Cat}$ in a manner very similar to that of Ub.wt (Fig. 3a), and also, the phage-derived UbVs 2.1^{PH} and 2.12^{PH} (Supplementary Fig. 6). The Cα atoms of the USP and Ub moieties in the UbV.2.6 and Ub.wt complex structures superposed with RMSD of 0.31 Å. The structure revealed a large intermolecular interface with 1833 and 1664 $Å^2$ of surface area buried on UbV.2.6 and $USP2^{Cat}$, respectively, and the UbV.2.6 side of the interface was centered on a triad of substituted residues (Cys^6, Arg^{11}, Cys^{12}) that were most important for enhanced inhibitory activity relative to Ub.wt (Fig. 3b). Notably, the interactions mediated by the side chains of Cys^6 and Arg^{11}, which together accounted for most of the enhanced activity of UbV.2.6 (Fig. 1c), differ substantially from those mediated by the corresponding side chains in Ub.wt (Fig. 3c). Specifically, the side chain of Cys^6 in UbV.2.6 makes hydrophobic contacts with the side chains of Phe^{462*} and Phe^{489*} (USP2 residues are indicated by asterisks), whereas the side chain of Lys^6 in Ub.wt makes a salt bridge with Asp^{466*} and a hydrogen bond with the main chain oxygen of Leu^{461*}. Arg^{11} in UbV.2.6 forms a hydrogen bond with the main chain oxygen of Val^{467*} and a salt bridge with the side chain of Asp^{466*}, whereas Lys^{11} in Ub.wt points away from the interface with USP2. Taken together, the mutational and structural analyses revealed that a triad of substituted residues in UbV.2.6 forms the center of the interface with USP2, and the side chains of Cys^6 and Arg^{11} substantially alter hydrophobic packing and hydrogen bonding to enhance the binding affinity and inhibitory potency of UbV.2.6 relative to Ub.wt.

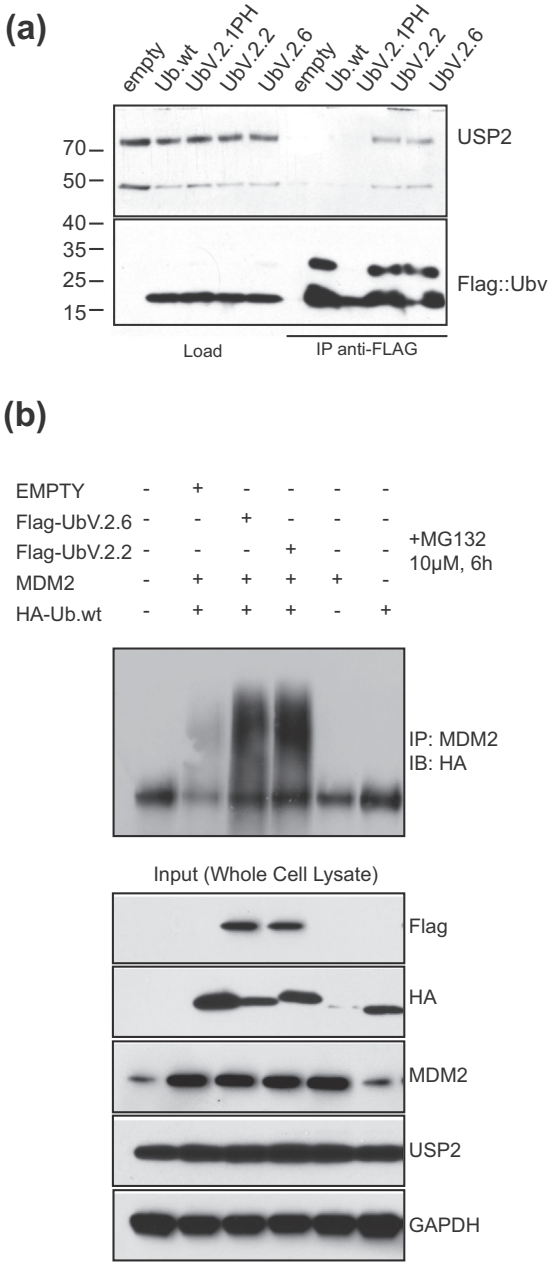

Fig. 2. Y2H-derived UbVs bind and inhibit USP2 in HEK293T cells. (a) Flag-tagged UbVs co-immunoprecipitate endogenous USP2. HEK293T cells were transfected with vectors to express the Flag-tagged UbVs or controls indicated across the top. Flag-tagged UbVs were immunoprecipitated from cell lysates with an anti-Flag antibody, and proteins were separated by SDS-PAGE and probed by Western blotting with antibodies to the proteins indicated on the right. Molecular weight standards are indicated on the left. (b) UbVs inhibit deubiquitination of MDM2 by USP2. HEK293T cells were transfected with an empty vector control or vector to express flag-tagged UbV.2.2 or UbV.2.6, and vectors to express HA-tagged Ub.wt and MDM2. MDM2 was immunoprecipitated from cell lysates, and proteins were separated by SDS-PAGE and probed by Western blotting with anti-HA antibody to detected HA-tagged Ub. Input whole cell lysate was probed with antibodies to the proteins indicated on the right.

Discussion

Targeting DUBs and other components of the UPS holds considerable promise for the development of therapeutics. DUBs have been implicated in many diseases including immune disorders, neurodegeneration and cancer [24–26]. However, the clinical success of UPS inhibitors lags behind efforts aimed at targeting phosphorylation and other post-translational modifications [7,8,10]. Hence, there is an urgent need for approaches aimed at interrogating specific

Table 2. Crystallographic data collection, processing and refinement statistics

	UbV.2.6-USP2
Data collection	
Space group	*C*2
Wavelength (Å)	1.5418
Cell dimensions	
a, *b*, *c* (Å)	159.98, 58.09, 46.84
α, *β*, *γ* (°)	90, 98.12, 90
Resolution range (Å)	50–2.34
R_{sym}	0.065 (0.149)
CC (1/2)	(0.961)
Total no. of observations	57,873
Total no. unique observations	18,044 (1628)
Mean [$(I)/\sigma(I)$]	31.5 (8.6)
Completeness (%)	99.0 (90.8)
Multiplicity	3.2 (2.4)
Refinement	
Resolution (Å)	37.76–2.34
No. of reflections	17,912
R_{work}/R_{free}	17.6/22.4
No. of atoms	
Protein	3172
Ligand/ion	11
Water	156
Average *B*-factors	
Protein	30.29
Ligand/ion	52.54
Water	31.97
R.m.s.d.	
Bond length (Å)	0.002
Bond angles (°)	0.46
Ramachandran statistics	
Residues in favored regions (%)	95.73
Residues in allowed regions (%)	3.77
Residues in disallowed regions (%)	0.5

Statistics in brackets are for highest-resolution shell (2.42–2.34 Å).

components of the UPS to enable target validation that facilitates drug development. To address this need, our group has employed UbVs as a general means to target DUBs and other UPS enzymes [11,12]. Phage display has enabled the targeting of many DUBs, but the technology has been limited to those enzymes that can be purified in a stable and active form, and some inhibitors that function *in vitro* do not work effectively in cells [11,12]. To circumvent these limitations, we developed a Y2H platform that enables the selection of tight and specific UbV inhibitors in an *in vivo* environment without the need for protein purification.

Our Y2H system comprises four reporters—*lacZ*, *HIS3*, *yEGFP* and *URA3*—which allow for precise control of selection stringency and virtually eliminate false positives. Furthermore, the use of the *yEGFP* reporter eliminates the use of labour intensive and costly plate-based selections. The *yEGFP* reporter can be combined with auxotrophic selection in liquid media, and interactors can be isolated rapidly by FACS. Another key feature is a new Y2H prey vector that is compatible with the Gateway® cloning system and is amenable to mutagenesis protocols that require the generation of single-stranded DNA. This allows for the facile generation of large combinatorial libraries, using single-stranded mutagenesis strategies that have been optimized for efficient construction of large phage-displayed libraries [20].

We used the Y2H platform to engineer potent inhibitors of USP2 that function in human cells, a result that was not achieved by phage display. Notably, the mutations derived by Y2H differed significantly from those found in phage-derived UbVs. Furthermore, we found that only the Y2H-derived UbV.2.6 was able to inhibit endogenous USP2 in human cells. While USP2 was the focus of this study, the Y2H screening platform can be readily adapted to target any number of DUBs and other UPS enzymes, and thus, our results establish Y2H screens as a powerful approach for the development of UbV inhibitors. However, phage display can access much larger libraries that can be used in pooled selections to enable high-throughput selections against hundreds of targets in parallel [27,28]. In contrast, the smaller libraries accessible with Y2H require screening protocols that are not readily amenable to high-throughput selections against many targets in parallel. Thus, the phage display and Y2H approaches possess complementary strengths and weaknesses, and we envision that Y2H will provide a valuable alternative for targeting UPS components that prove recalcitrant to phage display.

Finally, we anticipate that the UbV inhibitors described here will serve as useful tools for further investigating the function of USP2 in both normal and diseased cellular states. Moreover, as described in detail elsewhere [29], the general UbV technology will aid drug discovery efforts in the UPS in multiple ways. First, the ability to directly target enzyme active sites in live cells with small-molecule mimetics will enable target validation with much greater precision than is possible with RNA and gene knockout approaches. Second, structural studies of UbVs in complex with UPS enzymes provide insights into the molecular interactions that promote affinity and specificity, which could be applied to drug design. Finally, UbVs could serve as ideal binding partners for UPS components to enable high-throughput chemical screens to detect small-molecules that can displace UbVs and could thus be candidates for drug development.

Materials and Methods

Y2H reporter strain construction

The Y2H GFP reporter strains Y14648 and Y14649 were constructed by replacing the ADE2 chromosomal region of Y8930 and Y8800 with

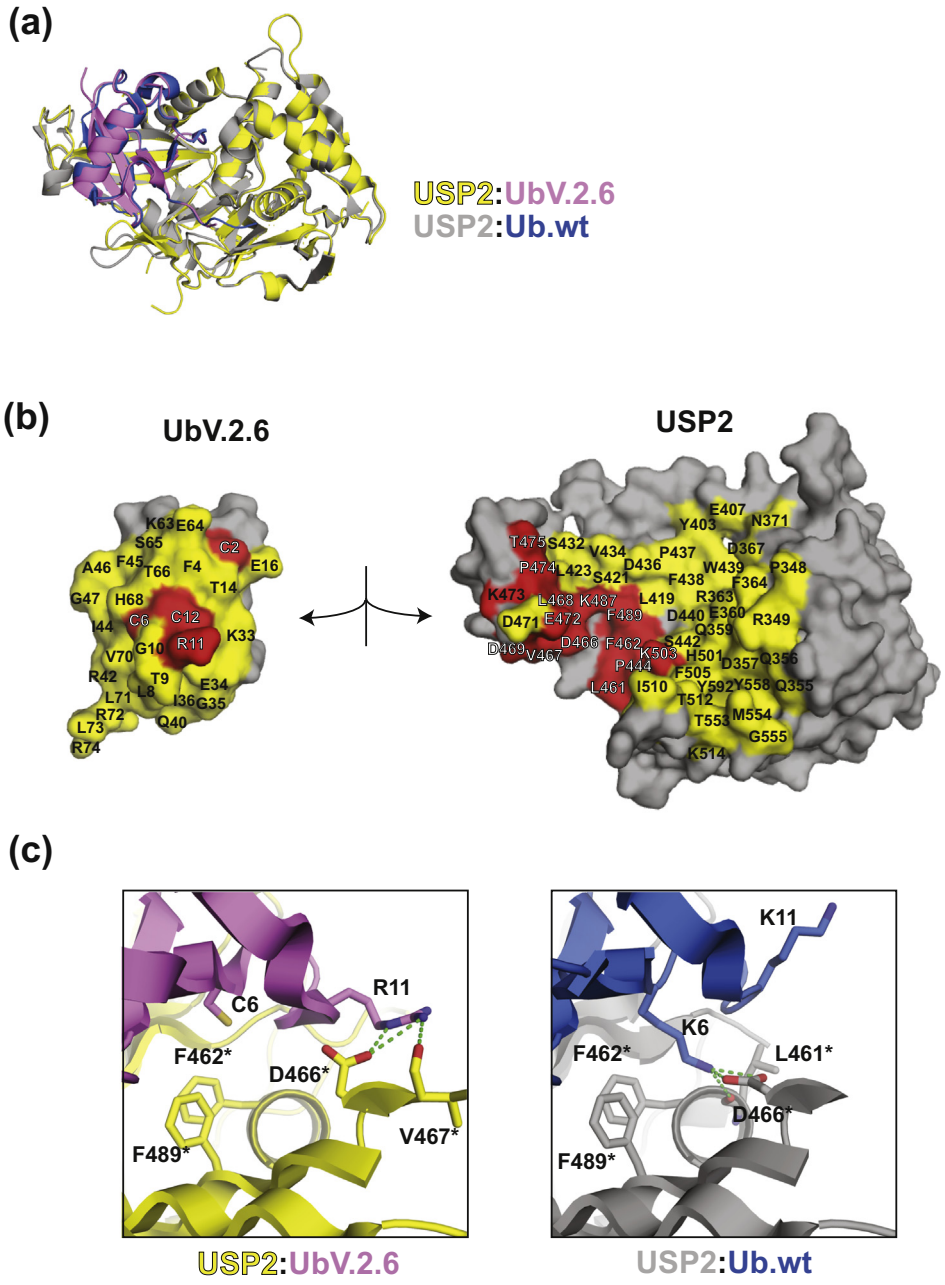

Fig. 3. The crystal structure of UbV.2.6 in complex with USP2. (a) Superposition of the structures of UbV.2.6 (magenta) bound to USP2 (yellow) and Ub.wt (blue) bound to USP2 (gray) (PDB entry: 2HD5). (b) Open book view of the complex between UbV.2.6 (left) and USP2 (right). The proteins are shown as molecular surfaces with non-contact residues colored gray. Residues on UbV.2.6 that are substituted or conserved relative to Ub.wt, and residues on USP2 that contact substituted or conserved residues on UbV.2.6, are colored red or yellow, respectively. (c) Detailed views of the molecular interactions between USP2 and the substituted residues Cys^{6} and Arg^{11} of UbV.2.6 (left) or the corresponding residues Lys^{6} and Lys^{11} of Ub.wt (right). Molecules are colored as in panel a.

yEGFP—kanamycin gene resistance cassette using PCR-based direct gene replacement. G418-resistant transformants were identified by plating cells on YPD + G418 (400 mg/L). Colonies were picked after 72 h and used as a reporter strain to determine EGFP fluorescence. To confirm the functionality of the yEGFP reporter, bait-tagged $USP2^{FL}$, and its cognate prey tagged UbV binder $UbV.2.1^{PH}$ (positive control) or empty plasmid (negative control), were transformed into the newly generated strains, Y14648 and Y14649, *via* lithium acetate and polyethylene glycol (Supplemental Table 1) [30]. Successfully transformed cells

were identified through plating cells on SD – Leu, – Trp selective media. After 72 h, colonies were picked and assessed for their ability to express EGFP using confocal microscopy. The colonies that produced the brightest EGFP signal were selected when expressing the positive control, and no EGFP with the negative control was selected.

Y2H bait and prey expression constructs and strains

A panel of 41 different DUBs and E2s from the Human ORFeome Collection V8.1 were cloned into the Y2H prey vector, pDEST32 *via* Gateway Cloning™ (Supplemental Table 2). To facilitate reciprocal testing of UbVs isolated in Y2H screens, all DUBs were cloned into the Y2H prey vector pDEST22 tagged with the AD of the Gal4 TF. All constructs were confirmed through restriction digest, using XhoI and SacI, and DNA sequencing. Strains harboring the resulting constructs were generated through transformation *via* lithium acetate and polyethylene glycol into the indicated yeast strain [30]. Successfully transformed cells were identified through plating cells on SD – Leu, – Trp selective media after 72 h.

Site-directed mutagenesis and library generation

The gateway-compatible GAL4 prey vector pDEST314 was generated by inserting the Gateway Cloning™ compatible GAL4-activation domain from pDEST22 into the yeast expression vector, pRS314 using standard cloning techniques. Briefly, the gateway-compatible Y2H cassette from pDEST22 was amplified using the primers F: CCGATCG ATATCCTTTTGTTGTTTCCGGGTGTA and R: CCGGGTACCCCGGTAGAGGTGTGGTCAATAA-GAG, and sub-cloned into the ClaI and KpnI restriction cloning sites found within pRS314. Successful constructs were identified *via* DNA sequencing.

A modified form of Ub that incorporated two stop codons and an ApaI restriction site into the region to be mutagenized was then transformed into pDEST314 using Gateway Cloning™. This was used as a template for oligonucleotide-directed mutagenesis, as previously described [11]. Variations were introduced at positions 2, 6, 11 and 12 of Ub. Mutagenic oligonucleotides were designed to replace positions to be scanned with degenerate NNK codons (N = A/G/C/T, K = G/C) that collectively code for all 20 natural amino acids (NP_USP2_R1: AAAAAAGCAGGCT C G A T G N N K A T T T T C G T G N N K A C C C TTACGGGGNNKNNKATCACCCTCGAGGTTGAA). Each mutagenesis reaction was electroporated into ElectroMax DH10B *Escherichia coli* and each yielded a library of $>10^5$ unique members. Resulting Libraries were extracted using PureLink HiPure Plasmid Maxiprep kit. UbV libraries were transformed into Y14648 *via* lithium acetate and polyethylene glycol yielding a library $>10^5$ unique members [29]. Resulting yeast cells were plated for single colonies onto 50 × 150-cm plates consisting of SD – Leu, – Trp media, scraped, pooled and frozen in 20% glycerol. Pooled library stocks were stored at – 80.

Mating and Y2H selection

To mate, cells expressing bait-tagged proteins were grown overnight in a shaking incubator to saturation (OD_{600} ~ 12), in 10 mL of liquid SD – Leu. Cultures were then diluted to early log phase and grown for an additional 3 h to a final OD ~ 0.6 in 50 mL of liquid SD – Leu media. Next, 5×10^7 cells expressing bait were mixed with 2.5×10^8 thawed library cells. Mating mixtures were transferred onto 40-mm mixed cellulose filters and incubated for 5 h at 30 °C on YEPD solid media. Cells were collected in 10 mL SD media lacking Leu and Trp. Serial dilutions on SD – Leu, SD – Trp and SD – Leu, – Trp were used to assess mating efficiency, mating efficiencies varied from 10% to 20% indicating a 30-fold to 60-fold coverage of the library per screen. Remaining cells were either subjected to (A) His selection by plating on solid SD – His, – Leu and – Trp + 100 mM ATZ or (B) EGFP selection (see below).

Resulting diploids were collected and grown overnight to an OD_{600} of ~ 2 in a shaking incubator, in 500 mL SD – Leu, – Trp, – His liquid media. 3×10^8 cells were pelleted and resuspended in 750 µL PBS for flow cytometry analysis. FACS Ariaii flow cytometer from Becton Dickson (San Jose, CA) was used to analyze the EGFP signal. Excitation of EGFP fluorescence was carried out at 488 nm and subsequently collected *via* 530/30-nm bandpass filter. FSC and SSC were used to gate the yeast single-cell population. The typical sample size was 2 million cells per measurement unless specified otherwise. Data analysis was performed using the FlowJo software.

EGFP expressing cells were collected and grown overnight to saturation in 10 mL SD – Leu, – Trp, – His liquid media and plated for single colonies on SD – Leu – Trp media.

Sequence analysis

The occurrence of each amino acid at each scanned position was corrected for bias by dividing the counts by the number of codons for that amino acid contained within the NNK degenerate codon. Normalized sequences were used to produce an alignment in LOGOS consensus format. Bits scores at position I were calculated according to the formula: $R_i = \log_2 20 - (H_i - en)$, where H_i, Shannon entropy at position i, $= -\Sigma f_{a,i} \times \log 2 f_{a,l}$, and $f_{a,i}$ is the relative frequency of amino acid, a, at position

i. Small sample correction, en, was assigned as 0, so that bits scores ranged from 0 to 4.32 ($log_2 20$).

Protein purification

Selected UbVs were cloned into pDEST53 *via* Gateway cloning, resulting in an open reading frame encoding a fusion protein consisting of a hexa-Histidine tag, followed by an UbV. The plasmids thus generated was transformed into *E. coli* BL21(DE3), and resulting transformants were processed *via* using standard techniques. IPTG (Bioshop, Canada) addition to a final concentration of 0.5 mM at mid-log phase was used to induce protein expression. After an overnight incubation at 18 °C, cell pellets were harvested at 12,200*g* for 10 min and lysed. Protein purification was done *via* Ni-NTA metal-affinity resin (Qiagen, Valencia, CA, USA) as per the manufacturer's guidelines. Next, polyacrylamide gel electrophoresis was used to determine the purity of eluted fractions. Proteins were dialyzed to the experimental buffer, and estimation of protein concentrations was carried out by calculating the absorption at 280 nm (Nanodrop 1000, Thermo Scientific, Rockford, IL, USA).

USP2 activity and inhibition assays

With Ub-amido-4-methylcoumarin (Ub-AMC) substrate (Boston Biochem, Boston, MA), assays were performed in assay buffer [50 mM Hepes (pH 7.5), 0.01% Tween 20, 10 mM dithiothreitol (DTT)] with 1 mM substrate, 7.5 nM USP2 and serial dilutions of UbV. USP2 and UbV were mixed in assay buffer and incubated at room temperature for 2 min prior to the addition of Ub-AMC. Release of fluorogenic AMC was monitored at 460 nm (excitation at 360 nm) for 30 min in a Synergy2 plate reader (BioTek Instruments, Winooski, VT). IC_{50} was defined as the concentration of UbV that inhibits 50% of USP2 activity and was fitted using the sigmoidal 4PL equation in GraphPad Prism software.

With Ub-rhodamine110 (Ub-Rh110) substrate (Boston Biochem, Boston, MA), assays were performed in assay buffer [PBS (pH 7.5), 0.01% Tween 20, 5 mM DTT] with 1 μM substrate, 0.5–5 nM DUB and serial dilutions of UbV. DUB and UbV were mixed in assay buffer and incubated at room temperature for 20 min prior to the addition of Ub-Rh110. Release of fluorogenic Rh110 was monitored at 535 nm (excitation at 485 nm) for 30 min in a SpectraMax M5e plate reader (Molecular Devices). The initial reaction velocities (nM/s) were determined for each UbV concentration, plotted *versus* UbV concentration, and fitted with XLFit (IDBS software) using a four-parameter logistical fit to determine the IC_{50}, the concentration of UbV that inhibited 50% of DUB activity.

CD spectroscopy assays

CD spectra were recorded on a Jasco J-810 spectropolarimeter using a cylindrical quartz cuvette with a 1-mm pathlength, 0.2-nm step resolution with 1.0-nm bandwidth, and a scan speed of 50 nm/min. Each spectrum was averaged over five measurements and corrected for the appropriate buffer baseline. Spectra for 40 μM Ub.wt or 30 μM UbV were measured in assay buffer (50 mM NaF, pH 7.5) at wavelengths of 197–260 nm for experiments at 37 °C or 216–260 nm for experiments at 90 °C or in 6 M GuHCl.

Thermostability of 40 μM protein was measured using the CD signal at a wavelength of 220 nm, and the temperature was increased from 20 to 90 °C at a rate of 1 °C/min using a peltier system to control temperature (JASCO PTC-423S). The ellipticity was plotted *versus* temperature and fit to a coarse lowess curve using Prism 7. Chemical stability of 30 μM protein was measured using the CD signal at a wavelength of 220 nm and at 20 °C, across a range of GuHCl concentrations (0–6 M). The CD signal was normalized to the signal at 0 M GuHCl, and the fraction of unfolded protein was plotted against GuHCl concentration and fit to a four-parameter model variable slope using Prism 7.

Co-immunoprecipitation assay to assess USP2 activity *in vivo*

Cell culture

HEK293T cells were cultured in Dulbecco's modified Eagles medium supplemented with 10% fetal bovine serum, 100 U/mL of penicillin and 100 μg/mL of streptomycin. Cells were maintained at 37 °C and 5% CO_2.

Transient cell transfection, immunoprecipitation and immunoblotting

To transiently express proteins in HEK293T cells, UbVs 2.2 and 2.6 were cloned into pDEST-pcDNA3.1/nFLAG vector (Gateway Cloning). Wild-type Ub was cloned into pDEST-pcDNA3.1/nHA vector (HA-Wt-Ub), and MDM2 was obtained from Addgene (No. 16233). All clones were sequence verified. HEK293T cells were grown to 60%–70% confluency on 6-well plates and transfected with 1 or 2 μg UbV or control plasmid (Empty vector), 1 μg of MDM2 and 0.5 μg of HA-WT-Ub using the Xtreme-GENE transfection reagent (Roche 06365809001) according to the manufacturer's instructions.

Cells were harvested 2 days post-transfection, washed in PBS and resuspended in lysis buffer [150 mM NaCl, 50 mM Tris (pH 8.0), 1% NP40, 4.5 mM Na_3VO_4, 4.5 mM sodium pyrophosphatase, 22.5 mM NaF, Halt Protease Inhibitor Cocktail

(Thermo scientific 78430)]. Lysates were centrifuged at 4 °C for 10 min at 12,000 rpm. The supernatant was transferred to a new tube, and protein concentration was determined by Bradford assay. For the immunoprecipitation assay, the lysates were incubated with anti-MDM2 antibody overnight at 4 °C followed by 2-h incubation with protein A/G agarose beads (No. 20423, Thermo Scientific). The agarose pellets were washed three times in lysis buffer. LDS sample buffer (NP0007, Life Technologies) with DTT was added to whole cell lysates and immunoprecipitated samples. Samples were heated at 70 °C for 10 min and loaded onto gels for standard Western blotting. Specific antibody list is indicated below.

Antibody list:

- o Anti-USP2, No. 8036, Cell Signaling.
- o Anti-GAPDH, No. 2118, Cell Signaling.
- o Anti-FLAG, F1804, Sigma.
- o Anti-MDM2, sc-813, Santa Cruz Technology.
- o Anti-HA, sc-7392, Santa Cruz Technology.

Co-immunoprecipitation assay to detect UbV interaction with endogenous USP2 in HEK293T human cells

Ub.wt, UbV.2.1^{PH}, UbV.2.2 and UbV.2.6 were cloned into pDEST-pcDNA3.1/nFlag vector (Gateway Cloning). All the constructs generated were sequence verified. HEK293T cells were cultures in 6-well culture plates to ~60%–70% confluence. Next, the cells were transfected with 1 µg of either UbV or control plasmid (pDEST-pcDNA3.1 Empty vector), using the XtremeGENE transfection reagent (Roche 06365809001) as per the manufacturer's instructions. Forty-eight hours after transfection, cells were harvested and washed in PBS and later resuspended in a cell lysis buffer [150 mM NaCl, 50 mM Tris (pH 8.0), 1% NP40, 4.5 mM NaVO4, 4.5 mM sodium pyrophosphatase, 22.5 mM NaF, Halt Protease Inhibitor Cocktail (Thermo scientific 78430)]. Cell lysates were then centrifuged at 4 °C for 10 min at 12,000 rpm. Following this, the supernatant was transferred to a new tube and protein concentration was estimated using the Bradford assay.

The cell lysates were then incubated with anti-FLAG antibody (F1804, Sigma), overnight at 4 °C followed by 2-h incubation with protein A/G agarose beads (No. 20423, Thermo Scientific). The agarose pellets were washed three times in lysis buffer. LDS sample buffer (NP0007, Life Technologies) with DTT was added to whole cell lysates and immunoprecipitated samples. Samples were heated at 70 °C for 10 min and loaded onto gels and later probed with a USP2 antibody (No. 8036, Cell Signaling), to visualize endogenous USP2 and an anti-Actin antibody (A2228, Sigma), as a loading control.

Protein expression and purification for crystallography

DNA fragments encoding UbV.2.2, UbV.2.6 or the catalytic domain of USP2 (residues 262–605) were cloned into the pET28a-LIC vector (GenBank EF442785) using the In-Fusion *CF* Dry-Down PCR Cloning Kit (Clonetech, Mountain View, CA, USA). Competent *E. coli* BL21 (DE3) cells (Invitrogen, Carlsbad, CA, USA) were transformed and grown at 37 °C in 2YT supplemented with 100 µg/mL ampicillin. At mid-log phase (OD600 = 0.6), the temperature was reduced to 18 °C, and after 1 h, protein expression was induced with 1 mM IPTG and the culture was incubated for 16 h at 18 °C. Cell pellets were collected by centrifugation at 12,000*g* for 20 min. For each liter of bacterial culture, pellets were resuspended in 25 mL lysis buffer (PBS, 0.1% Triton X-100, 2 mM $MgCl_2$, 0.4 mM PMSF OR 1 tablet of complete EDTA-Free protease inhibitors, 15 mg lysozyme, 2 µL benzoase nuclease). Cells were lysed using sonication (Branson Sonifier 450), and the cleared lysate was loaded onto NTA-resin (BD Biosciences) at 4 °C. After washing with was buffer (10 mL PBS and 10 mL PBS, 20 mM imidazole), proteins were eluted with elution buffer containing 150 mM imidazole and dialyzed overnight (UbVs in PBS and USP2^{cat} in 300 mM NaCl, 1 mM DTT).

To generate protein complexes, dialyzed UbV and the catalytic domain of USP2 were mixed for 1 h. Complexes were then concentrated to 3 mL at an approximate concentration of 20 mg/mL. Samples were further purified using size exclusion chromatography (Superdex 75 16/60 size exclusion column) eluting in 20 mM Hepes, 200 mM NaCl and 1 mM DTT. Samples were buffer exchanged into 20 mM Hepes, 50 mM NaCl and 1 mM DTT, concentrated to 10–20 mg/mL and flash frozen in 100 µL aliquots in liquid nitrogen.

Crystallography

The UbV.2.6-USP2^{cat} was crystallized in hanging drops using 24-well Linbro plates at 20 °C by mixing 1 µL of protein complex (13 mg/mL) with 1 µL of mother liquor [0.1 M MES buffer (pH 6), 12% w/v PEG 3350 and 0.2 M $NaSO_4$]. Crystals appeared after 7 days. Crystals were transferred to a cryoprotectant solution (mother liquor with 20% ethylene glycol) and flash frozen in liquid nitrogen. A single crystal data set was collected at – 180 °C on a home-source consisting of a Rigaku MicroMax-007 HF rotating anode generator coupled to a Rigaku Saturn 944 HG CCD detector. Data were processed by HKL-2000 [31]. Resolution of the collected data set was limited by the size of the CCD detector and detector distance to crystal. The structure was solved by molecular replacement using Phaser [32] and search models of Ub with the five C-terminal

residues removed [Protein Data Bank (PDB): 1UBQ] and USP2 (PDB: 2HD5). The structure was refined using Refmac [33]and PHENIX [34] with TLS parameters [35]and manual building in Coot [36]. Structural analysis was performed using The PyMOL Molecular Graphics System, Version 1.3, Schrödinger, LLC and Proteins, Interfaces, Structures, Assemblies (PISA) [37]. Figures were created using The PyMOL Molecular Graphics System, Version 1.3, Schrödinger, LLC.

Accession numbers

Coordinates and structure factors for the UbV.2.6-USP2 complex have been deposited in the PDB under the accession code 6DGF.

Supplementary data to this article can be found online at https://doi.org/10.1016/j.jmb.2019.02.007.

Acknowledgments

We would like to thank Helena Friesen, Kristin Kantautas and Priscilla Wang for their critical input on this research. This work was supported by Canadian Institutes of Health Research operating grants to Sachdev Sidhu (PJT-148510) and Frank Sicheri (FDN 143277).

Received 25 July 2018;
Received in revised form 1 February 2019;
Accepted 6 February 2019
Available online 11 February 2019

Keywords:
ubiquitin;
Ubiquitin Proteasome System;
ubiquitin variants;
Mdm2;
yeast two-hybrid

Abbreviations used:
Y2H, yeast two hybrid; DUB, deubiquitinating enzyme; USP2, ubiquitin-specific protease 2; Ub, ubiquitin; UbV, ubiquitin variant; ATZ, 3-amino triazole; HIS, histidine; Leu, leucine; Trp, tryptophan; EGFP, enhanced green fluorescent protein; UPS, Ubiquitin Proteasome System.

References

[1] D. Komander, The emerging complexity of protein ubiquitination, Biochem. Soc. Trans. 37 (2009) 937–953.
[2] S.M.B. Nijman, et al., A genomic and functional inventory of deubiquitinating, Enzymes (2005) 773–786, https://doi.org/10.1016/j.cell.2005.11.007.
[3] B. Cvek, Proteasome Inhibitors I. Short History of Bortezomib, The Proteasomal System in Aging and Disease, 109, Elsevier Inc., 2012
[4] L.H. de Wilt, a M, et al., Proteasome-based mechanisms of intrinsic and acquired bortezomib resistance in non-small cell lung cancer, Biochem. Pharmacol. 83 (2012) 207–217.
[5] K. Selvaraju, et al., Inhibition of proteasome deubiquitinase activity: a strategy to overcome resistance to conventional proteasome inhibitors? Drug Resist. Updat. 21–22 (2015) 20–29.
[6] P. Farshi, et al., Deubiquitinases (DUBs) and DUB inhibitors: a patent review, Expert Opin. Ther. Pat. 25 (2015) 1191–1208.
[7] C. Ndubaku, V. Tsui, Inhibiting the deubiquitinating enzymes (DUBs), J. Med. Chem. 58 (2015) 1581–1595.
[8] P. D'Arcy, S. Linder, Proteasome deubiquitinases as novel targets for cancer therapy, Int. J. Biochem. Cell Biol. 44 (2012) 1729–1738.
[9] F. Colland, The therapeutic potential of deubiquitinating enzyme inhibitors, Biochem. Soc. Trans. 38 (2010) 137–143.
[10] W. Zhang, et al., Generation and validation of intracellular ubiquitin variant inhibitors for USP7 and USP10, J. Mol. Biol. 429 (2017) 3546–3560.
[11] A. Ernst, et al., A strategy for modulation of enzymes in the ubiquitin system, Science 339 (2013) 590–595.
[12] I. Leung, A. Dekel, J.M. Shifman, S.S. Sidhu, Saturation scanning of ubiquitin variants reveals a common hot spot for binding to USP2 and USP21, Proc. Natl. Acad. Sci. 113 (2016) 8705–8710.
[13] M. Gorelik, S.S. Sidhu, Specific targeting of the deubiquitinase and E3 ligase families with engineered ubiquitin variants, Bioeng. Transl. Med. 2 (2017) 31–42.
[14] W.G. Nelson, A.M. De Marzo, S. Yegnasubramanian, USP2a activation of MYC in prostate cancer, Cancer Discov. 2 (2012) 206–207.
[15] A.L. Mahul-Mellier, et al., De-ubiquitinating protease USP2a targets RIP1 and TRAF2 to mediate cell death by TNF, Cell Death Differ. 19 (2012) 891–899.
[16] M.R. Boustani, et al., Overexpression of ubiquitin-specific protease 2a (USP2a) and nuclear factor erythroid 2-related factor 2 (Nrf2) in human gliomas, J. Neurol. Sci. 363 (2016) 249–252.
[17] I.C. Baines, P. Colas, Peptide aptamers as guides for small-molecule drug discovery, Drug Discov. Today 11 (2006) 334–341.
[18] M.B.T. Bickle, E. Dusserre, O. Moncorgé, H. Bottin, P. Colas, Selection and characterization of large collections of peptide aptamers through optimized yeast two-hybrid procedures, Nat. Protoc. 1 (2006) 1066–1091.
[19] A. Ciechanover, Tracing the history of the ubiquitin proteolytic system: the pioneering article, Biochem. Biophys. Res. Commun. 387 (2009) 1–10.
[20] R. Tonikian, Y. Zhang, C. Boone, S.S. Sidhu, Identifying specificity profiles for peptide recognition modules from phage-displayed peptide libraries, Nat. Protoc. 2 (2007) 1368–1386.
[21] P.L. Wintrode, G.I. Makhatadze, P.L. Privalov, Thermodynamics of ubiquitin unfolding, Proteins Struct. Funct. Bioinforma. 18 (1994) 246–253.
[22] S.Y. Lee, et al., Alanine scan of core positions in ubiquitin reveals links between dynamics, stability, and function, J. Mol. Biol. 426 (2014) 1377–1389.
[23] C.L. Wang, et al., Ubiquitin-specific protease 2a stabilizes MDM4 and facilitates the p53-mediated intrinsic apoptotic pathway in glioblastoma, Carcinogenesis 35 (2014) 1500–1509.

[24] S. Hussain, Y. Zhang, P.J. DUBs Galardy, Cancer 8 (2009) 1688–1697.
[25] P. Hanpude, S. Bhattacharya, A.K. Dey, T.K. Maiti, Deubiquitinating enzymes in cellular signaling and disease regulation, IUBMB Life 67 (2015) 544–555.
[26] J. Heideker, I.E. Wertz, DUBs, the regulation of cell identity and disease, Biochem. J. 465 (2015) 1–26.
[27] H. Huang, et al., Selection of recombinant anti-SH3 domain antibodies by high-throughput phage display, Protein Sci. 24 (2015) 1890–1900.
[28] H. Na, et al., A high-throughput pipeline for the production of synthetic antibodies for analysis of ribonucleoprotein complexes, RNA 22 (2016) 636–655.
[29] W. Zhang, M. Ben-David, S.S. Sidhu, System-wide modulation of HECT E3 ligases with selective ubiquitin variant probes, Curr. Opin. Struct. Biol. 45 (2017) 25–35.
[30] R.D. Gietz, R.A. Woods, Transformation of yeast by lithium acetate/single-stranded carrier DNA/polyethylene glycol method, Methods Enzymol. 350 (2002) 87–96.
[31] Z. Otwinowski, W. Minor, Processing of X-ray diffraction data collected in oscillation mode, Methods Enzymol. 276 (1997) 307–326.
[32] A.J. McCoy, et al., Phaser crystallographic software, J. Appl. Crystallogr. 40 (2007) 658–674.
[33] G.N. Murshudov, A.A. Vagin, E.J. Dodson, Refinement of macromolecular structures by the maximum-likelihood method, Acta Crystallogr. Sect. D Biol. Crystallogr. 53 (1997) 240–255.
[34] P.D. Adams, et al., PHENIX: a comprehensive Python-based system for macromolecular structure solution, Acta Crystallogr. Sect. D Biol. Crystallogr. 66 (2010) 213–221.
[35] J. Painter, E.A. Merritt, Optimal description of a protein structure in terms of multiple groups undergoing TLS motion, Acta Crystallogr. Sect. D Biol. Crystallogr. 62 (2006) 439–450.
[36] P. Emsley, K. Cowtan, Coot: model-building tools for molecular graphics, Acta Crystallogr. Sect. D Biol. Crystallogr. 60 (2004) 2126–2132.
[37] E. Krissinel, K. Henrick, Inference of macromolecular assemblies from crystalline state, J. Mol. Biol. 372 (2007) 774–797.